International Journal of Automotive Engineering, Vol. 9, No. 3, (2019), 3021-3032

Iran University of Science and Technology

International Journal of Automotive Engineering

Journal Homepage: ijae.iust.ac.ir

ISSN: 2008-9899

Pareto Optimal Multi-Objective Dynamical Balancing of a Slider-Crank Mechanism Using Differential Evolution Algorithm

Ghazal Etesami[1], Mohammad Ebrahim Felezi[2*], Nader Nariman-Zadeh[3]

[1,2,3] University of Guilan, Department of Mechanical Engineering

ARTICLE INFO

Article history:

Received: 25 May , 2019

Accepted: 28 July , 2019

Published: 1 Sept , 2019

Keywords:

Shaking forces and shaking moment

Slider-Crank Mechanism

Dynamical balancing

Multi-Objective Optimization

Differential Evolution-Algorithm

Pareto

A B S T R A C T

The present paper aims to improve the dynamical balancing of a slider-crank mechanism. This mechanism has been widely used in internal combustion engines, especially vehicle engines; hence, its dynamical balancing is important significantly. To have a full balance mechanism, the shaking forces and shaking moment of foundations should be eliminated completely. However, this elimination is usually impossible. Hence, in the current study, a multi-objective optimization is carried out to maintain the optimal balance of mechanism. The vertical and horizontal components of shaking forces and shaking moment are considered as objective functions. Also, the design variables are included the mass, the moment of inertia and the mass center location of mechanism links. The length of mechanism links is also considered constant for achieving a fixed slider course. The four-objective optimization is applied using a differential evolution algorithm. The optimization results are presented in Pareto diagrams as suitable tools for selecting a mechanism with desired characteristics according to the importance of each objective function. The optimal mechanism is finally introduced by the mapping method. The comparison of optimized mechanisms and the original one indicates a significant reduction of shaking forces and shaking moment as well as the reduction of energy consumption.

1. Introduction

Crank-slider mechanism has been widely used in internal combustion engines mostly in vehicle engines which transform the rotation into the translational motion. In recent years, mechanisms have worked at higher speeds. High speeds of an input link results in dynamic effects like link inertia, shaking forces and shaking moment leading to decreased kinematic and dynamic performance of mechanisms. Dynamic unbalancing of mechanisms is a common problem in mechanical engineering since it causes noise, attenuation and fatigue. The lower shaking forces and shaking moment leads to the higher life and performance. The present research aimed to reduce shaking forces and shaking moment by an optimization method. Optimization is an important design way in science and engineering problems [1]. When a mechanism dynamic equilibrium is formulated as an optimization problem, it is possible to use an optimization method for solving it. Therefore, the dynamical performance of a mechanism including shaking forces and shaking moment depends on the mass, moment of inertia, mass center position of moving

*Corresponding Author
Email Address: mefelezi@guilan.ac.ir
DOI: 10.22068/ijae.9.3.3021

[DOI: 10.22068/ijae.9.3.3021]

links; and it is highly necessary to have an optimum mass distribution for a proper dynamical balancing.

Multiple objective functions are defined in multi-objective optimization problems [2, 3] and should be simultaneously minimized or maximized. These objective functions almost act oppositely, so that improvement of one worsens another; hence, there is no unique point, which simultaneously makes all objective-functions optimal, but there is a set of responses which are known as optimum Pareto fronts or Pareto charts as the main difference in the general nature of single- and multi-objective problems. The term "Pareto" comes from the name of a famous Italian economist who first founded the theory of optimization with several objective functions in the economy.

Pareto theory [4] or the set of optimum points in objective function space in multi-objective problems is based on responses that are not superior than others. On the other word, changing the design variable vector in Pareto chart does not simultaneously improve all objective functions because at least an objective function gets worse. It should be noted that these non-superior responses are arranged at different layers that are formed based on the Pareto chart, and thus they include the most important responses. Felezi et al[5] used Pareto charts in most of their studies such as kinematic analysis of mechanisms. In recent years, an evolutionary method called the differential evolution algorithm (DE) [6] was introduced as a powerful and quick method for optimization problems in continuous spaces. Differential evolution searching algorithm is a new searching method. This algorithm was first introduced by Storn and Price in 1995. They found that this algorithm had a well power in non-derivable and non-linear objective functions. The applied optimization algorithm of the present paper was also utilized in previous studies in the kinematic optimization of mechanisms[7], but it has not been used in dynamic studies. Qiao et al. [8] used a differential evolution algorithm for optimum kinematic design of the spatial four-bar mechanism. An optimum synthesis of a four-bar mechanism by coupler control was performed using the differential evolution algorithm by Bulatovic et al. [9]. Lin et al. [10] proposed a new differential evolution algorithm with a combined mutation strategy for optimum synthesis of a path generating four-bar mechanism. Villarreal et al. [11] designed a five-bar parallel robot by a differential evolution algorithm. Shiacolus et al. [12] proposed an optimum synthesis of a six-bar mechanism using a differential evolution algorithm. Madavan et al. [13] extended the differential evolution algorithm for solving multi objective optimization problems by a Pareto-based approach. A great number of machine designers have proposed plans to solve the balance problem by classic methods such as redistributing the internal mass, adding supporting links, or new methods such as optimization methods. Feng et al. [14] designed 17 different types of eight-bar mechanism with joint clearances and proposed a method to eliminate shaking forces and shaking moment by the mass rearrangement. Ye et al. [15] introduced a method in which the mass redistribution was developed, so that the inertia torque effects were modeled in addition to the forces inertia by simple equivalent links leading to a complete balance of mechanism. Li [16]analyzed and formulated the sensitivity of shaking forces and moments for spatial mechanisms by changing mass parameters with a dynamic balance method that was resistant to fabrication process faults. The objective functions included shaking forces and torques that were obtained by the combination of identical weighting coefficients.

Arakelian et al. [17-19] presented a method using the redistribution of link mass for eliminating shaking forces and shaking moment both separately and simultaneously in a set of spatial mechanisms. Tepper and Lowen proposed a complete force balance of a spatial mechanism using equilibrium weights [20].

Esat and Bahai [21] also proposed a precise approval that if a mechanism could be completely balanced by the tepper and Lowen criteria, it was also possible to balance forces and torques simultaneously according to those criteria. Erkaya [22] investigated the best design variables to minimize shaking forces and shaking moment by a genetic algorithm and used three types of weighting coefficients to combine shaking forces and shaking moment. He considered all geometrical and mass parameters of a mechanism as design variables, and performed the optimization as a single objective. Chaudhary et al. [23] presented a single-objective optimization method using an equivalent point mass by a genetic algorithm for dynamical balancing of a crank-slider mechanism.

In previous studies [22, 23], weight coefficients were usually used to combine objective functions. The use of weight coefficients for objective functions with different dimensions and types

[DOI: 10.22068/ijae.9.3.3021]

makes the theoretical analysis of problems difficult. It is also difficult to select proper weight coefficients in order to combine objective functions; and results are generally dependent on the designer selection and affect values of objective functions. These kinds of problems are removed by a multi-objective optimization method. To obtain a complete balancing, it is necessary to eliminate both shaking forces and shaking moment, but a complete balancing of one leads to unbalancing of another. Shaking forces can be balanced by joining equilibrium weights to links. This is the same as classic methods, but this status increases mass and moment of inertia of the whole mechanism leading to increased shaking moment, jointed interaction, supported reaction and other mechanism dynamic values. Therefore, the multi-objective optimization method is also suggested to remove these problems.

The present research aimed to use a differential evolution algorithm for multi-objective dynamical balancing optimization of a crank-slider mechanism, and thus designer did not need to choose weight factors for combining the objective functions. In the research, this and algorithm was used for the multi-objective balancing optimization for a crank-slider mechanism; and the multi-objective optimization was simultaneously done considering four objective functions including horizontal and vertical components of shaking forces and shaking moment of the mechanism basis. Using the kinematic analysis and then formulating force and moment equations separately, shaking forces and shaking moment were obtained for considering them as objective functions. It is worth noting that previous studies [22, 23], which balanced mechanisms using the optimization method, length of moving links was assumed as design variables. In the crank-slider mechanism, the link length change can lead to the exit of mechanism from the intended purpose because the course length of slider changes in value, so length parameter exits from design variables; and lengths of links were assumed fixed. When the optimization is done, Pareto charts are presented for a pair combination of objective function, and results are compared as selected design points with the initial mechanism indicating a significant improvement in dynamical balancing compared with the main mechanism. Furthermore, calculations indicate that the final optimum mechanism significantly had reduced power consumption compared with the initial mechanism. This paper consists of the following sections; 1-kinematic and dynamic analysis of crank-slider mechanism, 2- describing the optimization process, 3- Results and discussion.

2. Kinematic and dynamic analysis of a crank-slider mechanism

The crank-slider mechanism is a special type of a four-bar mechanism. For more precision, a crank-slider mechanism is shown in figure 1. Kinematic analysis of mechanism consists of displacement, velocity and acceleration of moving links. Centers of mass of links are shown in equations 1 to 3 as basic equations for calculating velocity and acceleration of links. X_{Gi} and Y_{Gi} are momentous sites of center of mass of moving links in direction of X and Y axes. θ_2 is the angle of crank link, θ_3 shows the angle of coupler link relative to the x axis in CCW direction that is calculated from equation 4. Velocity and acceleration of the coupler link is obtained from the first and second derivatives of 1 to 3 equations. Angular velocity and acceleration of the coupler link is calculated from horizontal and vertical components of velocity and acceleration of points B and C of the rigid body. These quantities are shown in equations 5 and 6. For more clarification in describing equilibrium problem, the free body diagram of a crank-slider mechanism is shown in figure 2. The Joints forces are obtained by considering each link separately and writing Newton-Euler equations and change them into a set of matrix equations.

$$\begin{bmatrix} x_{G2} \\ y_{G2} \end{bmatrix} = r_{21} \begin{bmatrix} \cos(\theta_2 + \alpha_2) \\ \sin(\theta_2 + \alpha_2) \end{bmatrix} \quad (1)$$

$$\begin{bmatrix} x_{G3} \\ y_{G3} \end{bmatrix} = L_2 \begin{bmatrix} \cos\theta_2 \\ \sin\theta_2 \end{bmatrix} + r_{32} \begin{bmatrix} \cos(\theta_3 + \alpha_3) \\ \sin(\theta_3 + \alpha_3) \end{bmatrix} \quad (2)$$

$$\begin{bmatrix} x_{G4} \\ y_{G4} \end{bmatrix} = L_2 \begin{bmatrix} \cos\theta_2 \\ \sin\theta_2 \end{bmatrix} + L_3 \begin{bmatrix} \cos(\theta_3) \\ \sin(\theta_3) \end{bmatrix} \quad (3)$$

$$\theta_3 = \sin^{-1}\left[-\frac{L_2 \sin\Theta_2}{L_3}\right] \quad (4)$$

$$\dot{\theta}_3 = \dot{\Theta}_2 \frac{\partial\theta_3}{\partial\Theta_2} \quad (5)$$

$$\ddot{\theta}_3 = \alpha_2 \frac{\partial\theta_3}{\partial\Theta_2} + \dot{\Theta}_2^2 \frac{\partial^2\theta_3}{\partial\theta_2^2} \quad (6)$$

[DOI: 10.22068/ijae.9.3.3021]

$$\begin{bmatrix} r_{21x} & r_{21y} \\ r_{22x} & r_{22y} \\ r_{32x} & r_{32y} \\ r_{33x} & r_{33y} \end{bmatrix} = \begin{bmatrix} r_{21} & 0 & 0 & 0 \\ 0 & r_{22} & 0 & 0 \\ 0 & 0 & r_{32} & 0 \\ 0 & 0 & 0 & r_{33} \end{bmatrix} \times \begin{bmatrix} -\cos(\theta_2+\alpha_2) & -\sin(\theta_2+\alpha_2) \\ \cos(\theta_2-\beta_2) & \sin(\theta_2-\beta_2) \\ -\cos(\theta_3+\alpha_3) & -\sin(\theta_3+\alpha_3) \\ \cos(\theta_3-\beta_3) & \sin(\theta_3-\beta_3) \end{bmatrix} \quad (7)$$

$$\beta_2 = \cos^{-1}\left(\frac{\overline{BG_2}^2 + L_2^2 - \overline{AG_2}^2}{2\overline{BG_2}L_2}\right) \quad (8)$$

$$\beta_3 = \cos^{-1}\left(\frac{\overline{BG_3}^2 + L_3^2 - \overline{CG_3}^2}{2\overline{BG_3}L_3}\right) \quad (9)$$

$$r_{22} = \left(\overline{AG_2}^2 + L_2^2 - 2\overline{AG_2}L_2\cos\alpha_2\right)^{1/2} \quad (10)$$

$$r_{33} = \left(\overline{BG_3}^2 + L_3^2 - 2\overline{BG_3}L_3\cos\alpha_3\right)^{1/2} \quad (11)$$

$$\begin{bmatrix} -1 & 0 & 1 & 0 & 0 & 0 & 0 & 0 \\ 0 & -1 & 0 & 1 & 0 & 0 & 0 & 0 \\ r_{21y} & -r_{21x} & -r_{22y} & r_{22x} & 0 & 0 & 0 & 1 \\ 0 & 0 & -1 & 0 & 1 & 0 & 0 & 0 \\ 0 & 0 & 0 & -1 & 0 & 1 & 0 & 0 \\ 0 & 0 & r_{32y} & -r_{32x} & -r_{33y} & r_{33x} & 0 & 0 \\ 0 & 0 & 0 & 0 & -1 & 0 & 0 & 0 \\ 0 & 0 & 0 & 0 & 0 & -1 & 1 & 0 \end{bmatrix} \times \begin{bmatrix} F_{21x} \\ F_{21y} \\ F_{32x} \\ F_{32y} \\ F_{43x} \\ F_{43y} \\ F_{41y} \\ M_{21} \end{bmatrix} = \begin{bmatrix} m_2\ddot{x}_{G2} \\ m_2\ddot{y}_{G2} + m_2 g \\ I_{G2}\ddot{\theta}_2 \\ m_3\ddot{x}_{G3} \\ m_3\ddot{y}_{G3} + m_3 g \\ I_{G3}\ddot{\theta}_3 \\ m_4\ddot{x}_{G4} \\ m_4 g \end{bmatrix} \quad (12)$$

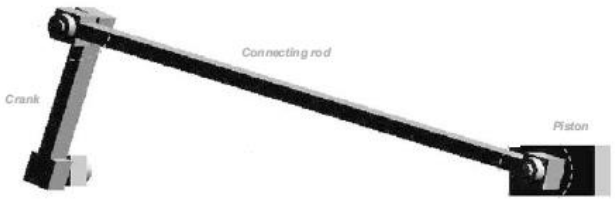

Figure 1: Crank-slider mechanism[24]

2.1. Differential evolution algorithm

Evolutionary algorithms are widely-used for solving multi-objective optimization problems because they use a set of initial populations. Therefore, most of the difficulties facing the multi-objective optimization existing in conventional methods have been modified in these algorithms. For instance, all optimum vectors are obtained by one-time run of program. Whereas, only a design vector is obtained in each run in other methods.

The important point is the maintenance of population variety in evolutionary algorithms and dispersion of optimized vectors in all solution domain. In recent years, researchers have found that the differential evolution algorithm has more capability in surveying searching space compared with genetic algorithm and the other conventional algorithms. Therefore, the present paper provided a multi-objective optimization algorithm based on a differential evolution algorithm that is described as below. In addition to general similarities of the differential evolution and other algorithms, the production method of new responses is a unique method in differential evolution algorithm.

In the differential evolution algorithm, the new population is generated based on crossover or mutation operators. If it was supposed to use two crossover and mutation operators simultaneously, results would be generated by crossover operator and then the mutation operator would be used. The method of mutation use and its step size are defined based on a probable distribution. Differential evolution algorithm is done according to the following stages:

1- Parametrical definition of problem and algorithm
2- Generating the initial population and evaluating its elements
3- Repetition of the following stages until the final condition is achieved.

[DOI: 10.22068/ijae.9.3.3021]

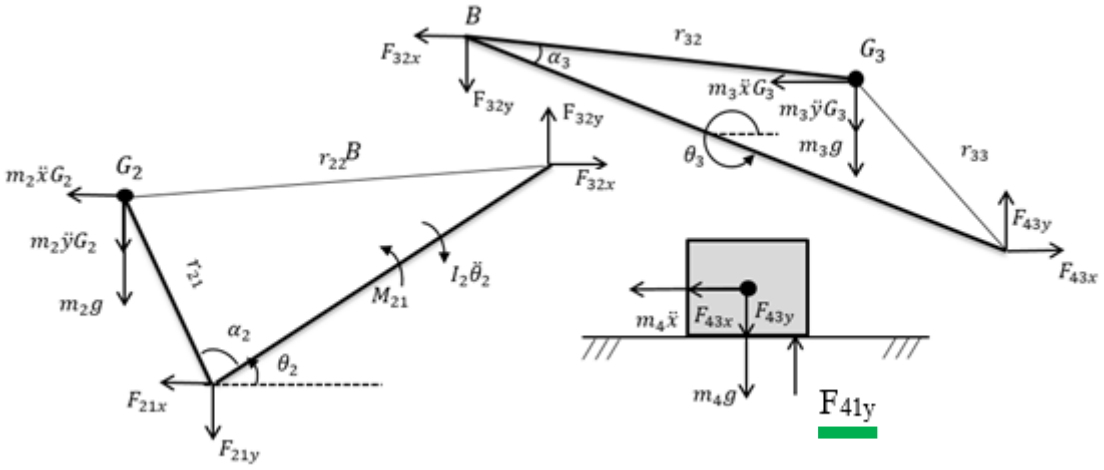

Figure 2: Force representation of crank-slider mechanism

The following stages are done for each element of population:

a) A temporary result is generated based on the mutation operator.
b) The new response is generated and evaluated based on the crossover operator.
c) If the new response is better than the previous one, the previous response is replaced by the new one, otherwise the previous one is preserved.
d) The best response is introduced as the output.
e) The uniform diversity criterion[5] is used at this stage. This operator compares two responses, and eliminate one of them if their distance is less than a desired limit in objective function or design variables space. Therefore, neighboring responses are eliminated and replaced with the new random population, and thus the searching space is widely surveyed. The generated populations are fronted, and these stages are repeated until the last loop. The first front is considered as the problem response in the last generation.

2.1.1. Method of creating a mutation and a temporary response

Assume that there are three responses of the previous population: *a*, *b* and *c*. We add a coefficient of *b-c* with *a* to get a new response. Therefore:

$$y = a + \beta\,(b\text{-}c) \qquad (13)$$

The obtained result sometimes may either lead to a better response or a worse response.

2.1.2. Cross-over method

A cross-over is introduced to increase the modified parametric vectors. To this end, the following test vector is created.

$$u_{i,G+1} = \begin{cases} y_{ji,G+1} & if\ randb \le P_{CR}\ \ or\ \ j = rnbr(i) \\ x_{ji,G}\ \ if\ \ randb > P_{CR} \end{cases} \qquad (14)$$

In randb (j), estimation j is a uniform random number generator with an output at the interval [0,1]. P_{CR} is a fixed cross-over at the interval [0,1] that should be determined by users. rnbr (i) is a randomly selected index belonging to 1,2, ..., D, that assures that $u_{i,G+1}$ takes at least a parameter of $v_{i,G+1}$.

2.2. Multi-objective optimization

In the multi-objective optimization, there is no method for simultaneous minimization or maximization of objective functions. Therefore, multi-objective optimization methods result in a set of optimal results that are not superior to each other. A set of all dominant solutions of the optimal front set and objective functions associated with them is called the Pareto front. Figure 3 shows an optimal Pareto front with two objective functions.

[DOI: 10.22068/ijae.9.3.3021]

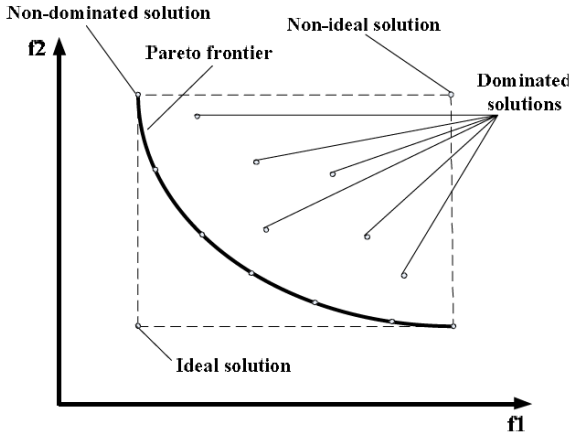

Figure 3: Optimum Pareto front of a multi-objective optimization problem[2]

3. Optimization process

As mentioned earlier, a complete balance of mechanism is obtained when all shaking forces and shaking moment are eliminated. Whereas, eliminating one increases another one. Due to this opposite behavior, the balance problem is defined as a multi-objective optimization problem with horizontal and vertical components of shaking forces and shaking moment as the objective functions.

The forces and torques, which are obtained from solving matrix equation 12, belong to only an angular position of the input link ($\theta_{2)}$. Since, values of torque and shaking forces should be obtained during a full circulation of a crank link as the input link in order to investigate the mechanism balance, we divide a complete 360-degree revolution or 2π rad into s points. S is set to 360 in this study. Therefore, the objective function is calculated for each point. The final objective functions are calculated by summating these values in a complete circulation as below:

$$F_{21x} = \sum_{n=1}^{s} (F_{21x}) \quad (15)$$

$$F_{21y} = \sum_{n=1}^{s} (F_{21y}) \quad (16)$$

$$F_{41y} = \sum_{n=1}^{s} (F_{41y}) \quad (17)$$

$$M_{sh} = \sum_{n=1}^{s} (x_4 \times F_{41y}) \quad (18)$$

It should be noted that the friction between slider and ground was neglected; hence, we sought to reduce F_{21x}, F_{21y} , $and\ F_{41y}$ as horizontal and vertical forces of basic joints of mechanism, and M_{sh} as the shaking moment. The objective functions are considered as below:

$$Min\ f(x) = \{F_{21x}, F_{21y}, F_{41y}, M_{sh}\ \} \quad (19)$$

Which are supposed to be minimized with a set of constraints. The constraints are the upper and lower limits of vector of design variables which are necessary for a mechanism design. These are defined as below:

$$X = [m_i\ I_{Gi} \alpha_i r_{21}\ r_{32}\ ] \quad (20)$$

The general process of problem solving is as follows:

I. start
II. Gaining the location, speed and acceleration of center of mass of each link
III. Entering the optimization process

It should be noted that Figure 4 shows the optimization process in further clarity as a flowchart.

α_i as $\alpha_1$and α_2 are the structural angles of moving links; m_i as m_1, m_2 and m_3 are the mass of moving links; I_{Gi} as I_{G2} and I_{G3} refer to the inertia of crank and coupler links of mechanism. r_{21} and r_{32} are the position vectors of crank and coupler links. The upper and lower bounds of design variables are adjusted according to the working space of mechanism, the link geometry, depth, thickness and length of each moving link.

[DOI: 10.22068/ijae.9.3.3021]

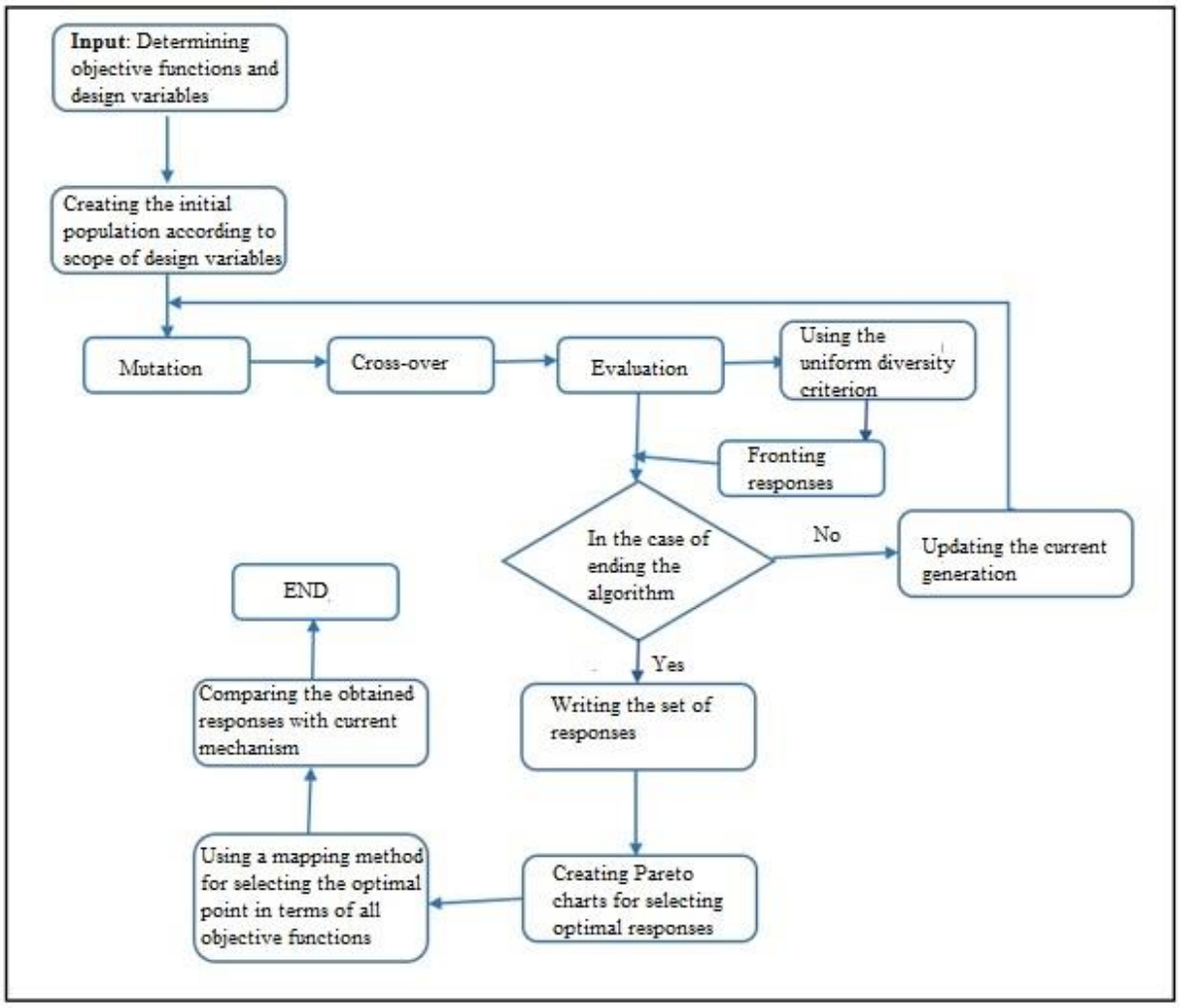

Figure 4: The overall process of solving the optimization problem of the present research

Table 1: The obtained values of design variables for different considered mechanisms

Row	Design variable	Mechanism A	Mechanism B	Mechanism C	Mechanism C_1	Mechanism C_2	Mechanism C_3	Mechanism C_4	Mechanism D	Mechanism E
1	m_2 (kg)	0.977	0.841	1992	1.33	2.317	2,014	2.039	2.489	2
2	I_{G2} (kgm^2)	0.039	0.041	0.036	0.017	0.025	0.0174	0.0336	0.027	0.03
3	α_2(Radian)	3.232	3.416	3.298	3.19	3.214	3.235	3,006	3.136	0
4	r_{21}(mm)	249	247.5	249.6	248.8	249.2	245.7	249	245	146
5	m_3 (kg)	1,004	1.003	1,004	1.005	1.385	3.978	1,008	1.014	3
6	I_{G3} (kgm^2)	0.004	0.004	0.007	0.003	0.004	0.003	0.004	0.0047	0.14
7	α_3(Radian)	2.89	0.037	3.282	3.478	3.433	3.452	3.465	3.402	0
8	r_{32}(mm)	101	364	191.8	154	0.187	106.4	108.4	193.5	214
9	m_4 (kg)	2.002	2.002	2	2009	2.002	2	2.007	2.001	4

Table 2: The obtained values of objective functions for different considered mechanisms

Objective functions	A	B	C	C_1	C_2	C_3	C_4	D	E (original mechanism)
F_{21x}	6776.62	8105.16	3424.34	5970.309	4642.96	11615.41	4679.604	3729.29	24060
F_{21y}	8311.73	4897.55	15235.07	9954.233	14456.72	24501.65	11148.25	13107.39	16970
F_{41y}	6664.27	10061.97	6417.31	6704.877	6412.665	5718.973	6697.932	6481.85	19580
M	62244.55	91998	55455.73	54297.78	51470.07	45754.46	56311.82	52496.16	178610

Table 3: The improvement percentage of objective functions compared to E (Original Mechanism)

[DOI: 10.22068/ijae.9.3.3021]

Objective functions	A	B	C	C_1	C_2	C_3	C_4	D
F_{21x}	72	66	86	75	81	52	81	85
F_{21y}	51	71	10	41	15	-44	34	23
F_{41y}	66	49	67	66	67	71	66	67
M_{sh}	65	48	69	70	71	74	68	71

4. Results and discussion

The present paper used a crank-slider mechanism for which shaking forces and shaking moment were theoretically calculated. The angular velocity of input link is considered to be constant and set to 60 rpm. The horizontal and vertical components of shaking force of the crank link (F_{21X}) and (F_{21y}), vertical shaking force of slider (F_{41y}) and the shaking moment (M_{sh}) are considered as the objective functions. In this section, Pareto charts and optimization results, which are obtained by differential evolution algorithm, are presented in binary space. The analyzed objective function pairs in this section are (F_{21x}, F_{21y}) ،(F_{21x}, F_{41y})، (F_{21x}, M_{sh}) ،(F_{21y}, F_{41y})، (F_{21y}, M_{sh}) and (F_{41y}, M_{sh}). All these pairs are minimized and the corresponding Pareto charts are presented. The differential evolution algorithm is used with the crossover operator equal to 0.3, and mutation step was randomly selected between 0.4 and 0.6. The responses are fronted by the uniform diversity operator; and the iteration number for the optimization process is considered 500.

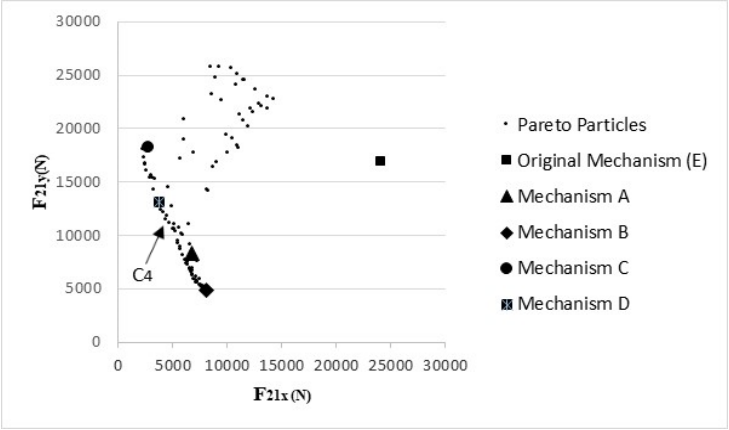

Figure 5: Pareto front of F_{21x} and F_{21y}

Figure 5 to 10 show Pareto charts of each two objective functions.

According to Pareto charts, decreasing an objective function increases another function. Therefore, the best possible combination of objective function pairs is obtained by selecting a group of design variables based on the Pareto front.

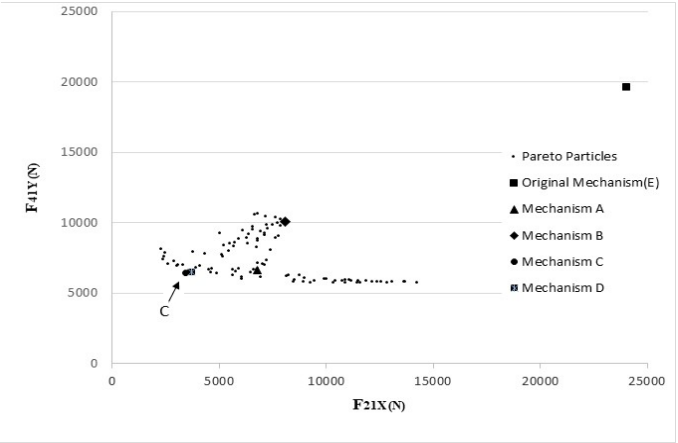

Figure 6: Pareto front of F_{21x} and F_{41y}

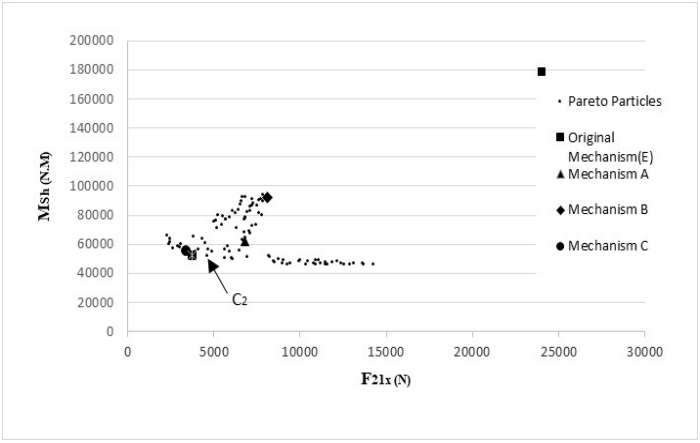

Figure 7: Pareto charts of each F_{21x} and M_{sh}

In other words, selecting any other group of design variables worsens the corresponding objective functions. This worse space is shown in right/above of Pareto curves in figures 5 to 10.

Figure 9 shows the Pareto front of two objective functions including the vertical force of crank link and the shaking moment. It is shown that the Pareto front provides the designer with many optimum points according to the opposed objective functions. This points are non-dominant, and the designer can select one of them based on his requirements. As shown, the vertical force of

[DOI: 10.22068/ijae.9.3.3021]

driver link is minimum for point B. There are design points between Pareto points with a significant improved objective function despite the other one with no considerable change, a trade-off can be performed between objective functions using these points. The C_1 point in figure 9 is a representative of a trade-off point. As seen in this figure, with a little increase of the shaking moment objective function, we move from the optimum point D to the optimum point C_1, and there is no significant change in shaking moment objective function from point C_1 to D, but the crank link decreases by 24% for the vertical force objective function. Therefore, the C_1 point can be a proper design point, since it is not significantly changed for an objective function, but it is improved for another objective function. Such a trade-off point can be obtained by the multi-objective optimization. It is also possible to find the trade-off point from other Pareto charts.

Figures 5 to 10 show Pareto charts of non-dominated points for objective function pairs. As shown, the optimum points A ،C_1 ، C_2، ،C_3 ،C_4 and C are chosen as trade-off points, respectively. None of dominant points, which are proposed by this Pareto charts, are significantly better than point E of the initial mechanism. Tables 1 and 2 present design variables of trade-off points of the four-objective optimization together with the corresponding objective function values for the initial mechanism.

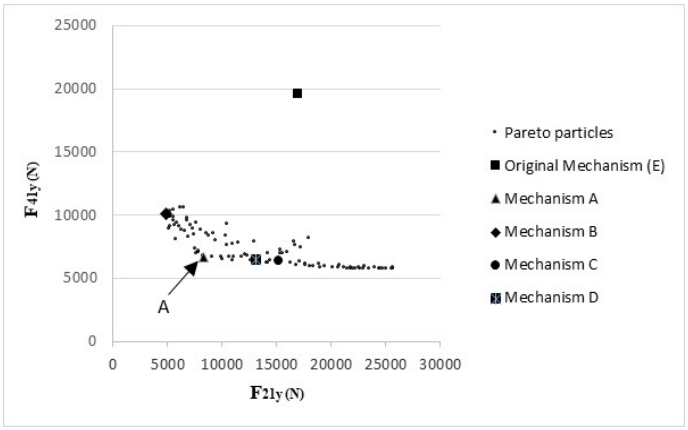

Figure 8: Pareto front of F_{21y} and F_{41y}

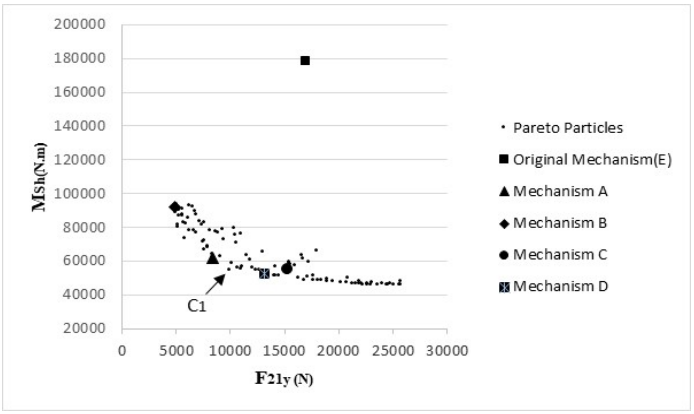

Figure 9: Pareto front of F_{21y} and M_{sh}

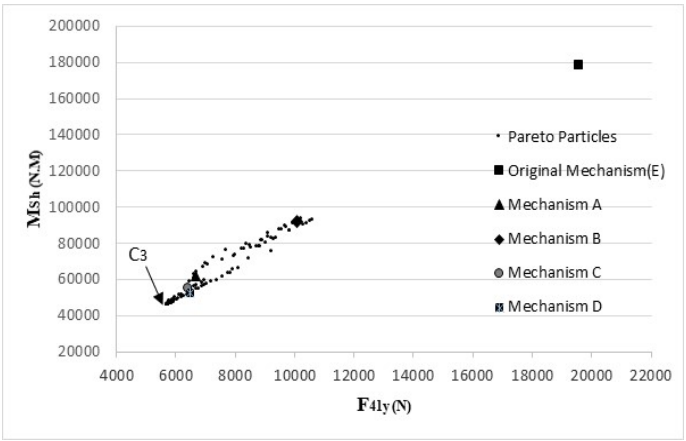

Figure 10: Pareto front of F_{41y} and M_{sh}

Finally, the purpose was to define an optimum point as the optimal result among all non-dominant points of the four-objective optimization, so that this point can satisfy all objective functions from this point of view.

In other words, all of optimum points, which were proposed in previous section, are acceptable in their corresponding objective function pairs space, but there is no reason that the proposed optimum point in a Pareto front (such as plane (F_{21x}, F_{21y})) also exists in another Pareto front (such as plane (F_{41y}, M_{sh})). To obtain this point, all values of objective functions of non-superior points were mapped in a range of 0 to 1. From the perspective of all objective-functions, the optimal point, which is called D, has the least summation of mapped objective functions. All of this points are non-dominant when all four objective functions are simultaneously considered. Therefore, designers can select any point according to their requirements. For more clarification of behavior of point D, Figure 11 shows the crank link compared with the original mechanism (point E) for each objective function in a complete revolution. These diagrams emphasize that forces and moments are significantly reduced and the mechanism balancing is successful by maintaining the length of links using this method. Furthermore, Table 3 presents the improvement in results of selected mechanisms compared to the original mechanism. On the other hand, the maximum value of input torque (M_{21}), which is necessary to produce the 60 rpm angular velocity for the original mechanism,

[DOI: 10.22068/ijae.9.3.3021]

is 3820 Nm. To produce such a moment, a motor with nominal power of at least 24001.06 w is needed according to equation 19.

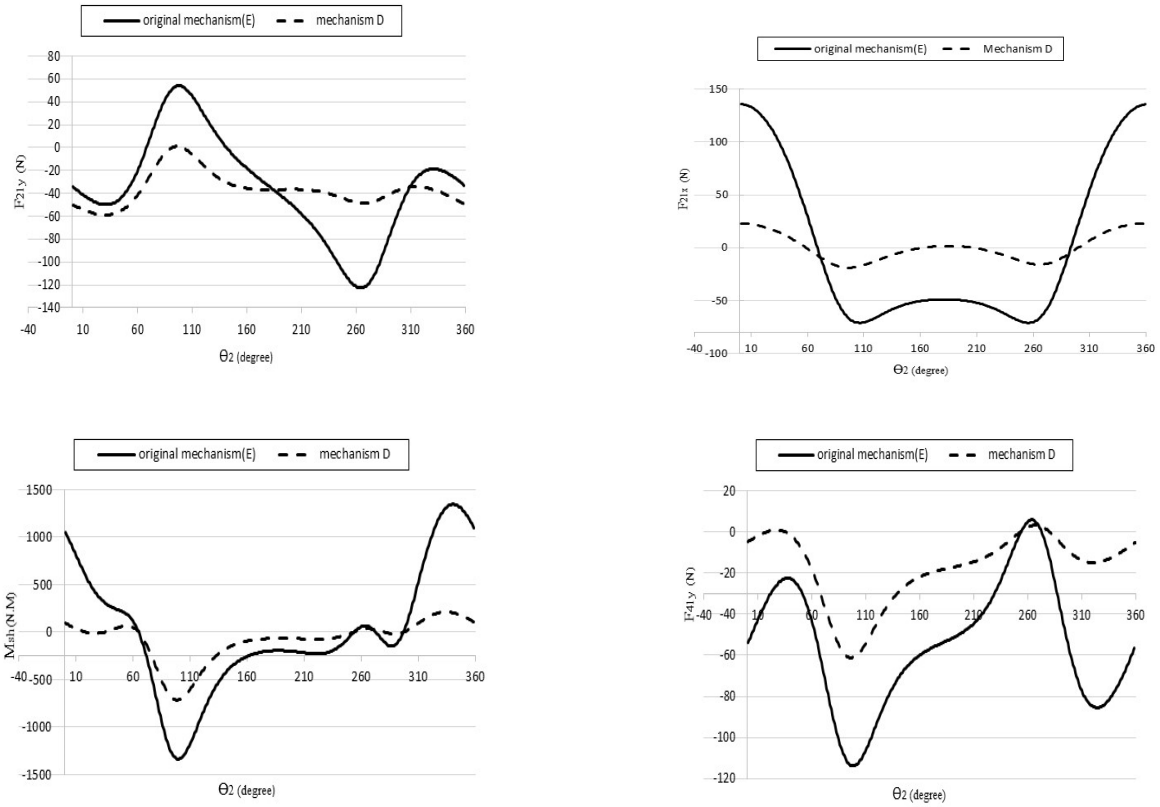

Figure 11: Behavior of objective functions of the final optimum mechanism (D) compared to the original mechanism (E) in one complete circulation of crank link

[DOI: 10.22068/ijae.9.3.3021]

Whereas, the maximum input torque is 1099 Nm in trade off point mechanism and it needs a motor with a nominal power of 6905 W. Therefore, the power consumption can be reduced by 71.23% leading to a 61545 KJ reduction in the energy consumption in an hour.

$$P = M_{21} \times \dot{\theta}_2 \quad (21)$$

5. Conclusion

In the present paper, the reduction of shaking forces and shaking moment of a crank-slider mechanism was done as a multi-objective problem solving. For achieving this goal, a theoretical model was used to study shaking forces and shaking moment. The angular velocity of driver link was set to 60 rpm. Objective functions were derived from Newton-Euler equations for mechanism links and they were combined in a system of equations. To solve the dynamical balancing problem of mechanism, a multi-objective differential evolution optimization method was used with fronting non-superior points. Mass and moment of inertia and mass centroid position of moving links except for the slider mass center were considered as design variables. Horizontal and vertical components of shaking forces and shaking moment were considered as objective functions. Multi-objective optimization results included some optimal design points that were presented in Pareto charts, and designers could choose points as the optimal design points depending on their needs. Given the identical importance of objective functions by mapping method, a point called trade-off point was obtained as the best result. The point decreased shaking forces and shaking moment by about 61.5% compared with the initial mechanism. For a better perception of results, graphs of objective functions of the trade-off point were presented compared with the initial mechanism for a complete revolution of the crank link. The use of an optimum mechanism with balanced shaking forces and shaking moment improved the desired performance of mechanism, reduced noise and destructive vibrations, and finally increased the useful life of mechanism. Despite the non- consideration of the power consumption of mechanism as the objective function, there were significant results in its reduction (about 71%). According to comparison of objective functions of the trade-off point and some other selected design points with the original mechanism, the method was highly efficient. It is suggested using this method for other mechanisms including robots and spatial mechanisms.

References

[1] S. S. Rao, Engineering optimization: theory and practice. John Wiley & Sons, (2009).

[2] A. Sedaghat and H. Kian, Multi-Criteria Optimization of a solar cooling system assisted ground source Heat Pump system, (in persian), Modares Mechanical Engineering, vol. 16, no. 1, (2016), pp. 51-62.

[3] C. A. C. Coello, G. B. Lamont, and D. A. Van Veldhuizen, Evolutionary algorithms for solving multi-objective problems. Springer, (2007).

[4] V. Pareto, Cours d'économie politique. Librairie Droz, (1964).

[5] M. E. Felezi, S. Vahabi, and N. Nariman-Zadeh, Pareto optimal design of reconfigurable rice seedling transplanting mechanisms using multi-objective genetic algorithm, nueral computing and applications, vol. 27, no. 7, (2016), pp. 1907-1916.

[6] R. Storn and K. Price, Differential evolution–a simple and efficient heuristic for global optimization over continuous spaces, Journal of global optimization, vol. 11, no. 4, (1997), pp. 341-359.

[7] A. A. Saghalaksari and M. E. Felezi, Optimal Path Design of Geared 5-bar mechanism using Differential Evolution Algorithm, International Journal Of Advanced Biotechnology And Research, vol. 7, (2016), pp. 1951-1959.

[8] F. L. Qiao and H. B. Miao, Notice of Retraction Optimization design for planar four-bar mechanism based on differential evolution, in *2010 Sixth International Conference on Natural*

[DOI: 10.22068/ijae.9.3.3021]

Computation, 2010, vol. 8, pp. 4131-4134: IEEE.

[9] R. R. Bulatović and S. R. Dordević, On the optimum synthesis of a four-bar linkage using differential evolution and method of variable controlled deviations, Mechanism and Machine Theory, vol. 44, no. 1, (2009), pp. 235-246.

[10] W. Lin and K. Hsiao, A new differential evolution algorithm with a combined mutation strategy for optimum synthesis of path-generating four-bar mechanisms, Proceedings of the Institution of Mechanical Engineers, Part C: Journal of Mechanical Engineering Science, vol. 231, no. 14, (2017), pp. 2690-2705.

[11] M. G. Villarreal-Cervantes, C. A. Cruz-Villar, J. Alvarez-Gallegos, and E. A. Portilla-Flores, Differential evolution techniques for the structure-control design of a five-bar parallel robot, Engineering Optimization, vol. 42, no. 6, (2010), pp. 535-565.

[12] P. Shiakolas, D. Koladiya, and J. Kebrle, On the optimum synthesis of six-bar linkages using differential evolution and the geometric centroid of precision positions technique, Mechanism and Machine Theory, vol. 40, no. 3, (2005), pp. 319-335.

[13] N. K. Madavan and B. A. Biegel, Multiobjective optimization using a Pareto differential evolution approach, (2002).

[14] G. Feng, Complete shaking force and shaking moment balancing of 17 types of eight-bar linkages only with revolute pairs, Mechanism and Machine Theory, vol. 26, no. 2, (1991), pp. 197-206.

[15] Z. Ye and M. Smith, Complete balancing of planar linkages by an equivalence method, Mechanism and Machine Theory, vol. 29, no. 5, (1994), pp. 701-712.

[16] Z. Li, Sensitivity and robustness of mechanism balancing, Mechanism and Machine Theory, vol. 33, no. 7, (1998), pp. 1045-1054.

[17] V. Arakelian, Shaking moment cancellation of self-balanced slider–crank mechanical systems by means of optimum mass redistribution, Mechanics Research Communications, vol. 33, no. 6, (2006), pp. 846-850.

[18] V. Arakelian and M. Dahan, Partial shaking moment balancing of fully force balanced linkages, Mechanism And Machine Theory, vol. 36, no. 11-12, (2001), pp. 1241-1252.

[19] V. H. Arakelian and M. Smith, Shaking force and shaking moment balancing of mechanisms: a historical review with new examples, Journal of Mechanical Design, vol. 127, no. 2, (2005), pp. 334-339.

[20] F. R. Tepper and G. G. Lowen, General theorems concerning full force balancing of planar linkages by internal mass redistribution, Engineering For Industry, vol. 94, no. 3, (1972), pp. 789-796.

[21] I. Esat and H. Bahai, A theory of complete force and moment balancing of planer linkage mechanisms, Mechanism and Machine Theory, vol. 34, no. 6, (1999), pp. 903-922.

[22] S. Erkaya, Investigation of balancing problem for a planar mechanism using genetic algorithm, Journal of Mechanical Science Technology, vol. 27, no. 7, (2013), pp. 2153-2160.

[23] H. Chaudhary and S. K. Saha, Balancing of shaking forces and shaking moments for planar mechanisms using the equimomental systems, Mechanism and Machine Theory, vol. 43, no. 3, (2008), pp. 310-334.

[24] S. Erkaya and I. Uzmay, Optimization of transmission angle for slider-crank mechanism with joint clearances, Structural Multidisciplinary Optimization, vol. 37, no. 5, (2009), pp. 493-508.

[DOI: 10.22068/ijae.9.3.3021]